

# Methane loss from $(\text{CH}_3)_3\text{O}^+$ : An asynchronous, concerted 1,2-alkane elimination

Charles E. Hudson, David J. McAdoo\*

Department of Neuroscience and Cell Biology, University of Texas Medical Branch, 301 University Boulevard,  
Galveston, TX 77555-1043, United States

Received 10 August 2005; received in revised form 8 November 2005; accepted 8 November 2005  
Available online 20 December 2005

## Abstract

To advance our understanding of 1,2-eliminations, ab initio and density functional theories are used to characterize the elimination of  $\text{CH}_4$  from  $(\text{CH}_3)_3\text{O}^+$ . The reaction begins with the extension of a CO bond. Near the transition state, the carbon of the moving methyl ( $\text{C}_{\text{Me}}$ ) begins to approach a hydrogen ( $\text{H}_i$ ) in another methyl, and the original  $\text{CH}_i$  bond begins to stretch. Finishing the transfer of  $\text{H}_i$  after the transition state is passed completes the elimination. At the transition state, more than half of the positive charge is on the moving methyl, so the initial phase of methane elimination resembles the beginning of heterolytic dissociation to  $^+\text{CH}_3 + \text{CH}_3\text{OCH}_3$ , a reaction that also occurs. There is no electron density overlap between the C and O at the transition state, but there is significant overlap density between  $\text{C}_{\text{Me}}$  and  $\text{H}_i$ . This and the charge distribution lead to classification of methane elimination as a concerted but highly asynchronous process rather than as being ion-neutral complex-mediated, in contrast to many alkane eliminations. The concertedness of this process probably arises from the threshold for partial dissociation of this system to an ion-neutral complex being much higher than the endothermicity for methane elimination.  
© 2005 Elsevier B.V. All rights reserved.

**Keywords:** Ab initio; Trimethyloxonium ion; 1,2-Elimination; Orbital symmetry; Ion-neutral complex

## 1. Introduction

The varied and unusual nature of their transition states has generated interest in 1,2- $\text{H}_2$  [1] and 1,2-alkane eliminations [2–4] from cations in the gas phase. This variety has been attributed [5,6] to the need to circumvent Woodward–Hoffmann barriers [7] to concerted 1,2-eliminations. Bond-breaking and bond-making for 1,2-eliminations are invariably quite asynchronous, being initiated either by CH or by CC bond stretching. Most 1,2-eliminations from cation radicals take place in essentially two steps through intermediate ion-neutral complexes [2,8–12], defined in this context as fragments that are held together by non-covalent attractions such that they can react with each other [9,12]. However, some closed shell cations undergo concerted, albeit asynchronous, 1,2-eliminations, the details of which vary with the system undergoing the elimination. At one extreme, loss of a carbon and four hydrogen atoms from the

tetramethyl ammonium ion appears to produce  $\bullet\text{CH}_3$  and  $\text{H}\bullet$  as separate fragments rather than as methane [13]. In other closed shell cations, H migrates through hypervalent configurations to attack and replace an existing bond [1,3–6,14–16]. The products of  $\text{CH}_4$  elimination from  $(\text{CH}_3)_3\text{O}^+$  are substantially lower in energy than those from the simple loss of methyl, a situation that might produce a concerted but nonsynchronous elimination [14]. It has been inferred from the appearance energy for methane elimination being close to that for  $^+\text{CH}_3$  formation that  $\text{CH}_4$  elimination from  $(\text{CH}_3)_3\text{O}^+$  is highly asynchronous, with a transition state strongly resembling a  $[\text{CH}_3^+ \text{CH}_3\text{OCH}_3]$  complex [17]. To extend our understanding of 1,2-eliminations by closed shell species, we here use theory [18] to characterize the transition state for  $\text{CH}_4$  elimination from  $(\text{CH}_3)_3\text{O}^+$ .

## 2. Results and discussion

### 2.1. Ground and transition state geometries

QCISD/6-31G\* theory produced a geometry for  $(\text{CH}_3)_3\text{O}^+$  with  $C_{3v}$  symmetry, the oxygen being pyramidal with COC bond

\* Corresponding author. Tel.: +1 409 772 2939; fax: +1 409 772 3222.

E-mail addresses: [cehudson@utmb.edu](mailto:cehudson@utmb.edu) (C.E. Hudson),  
[djmcadoo@utmb.edu](mailto:djmcadoo@utmb.edu) (D.J. McAdoo).

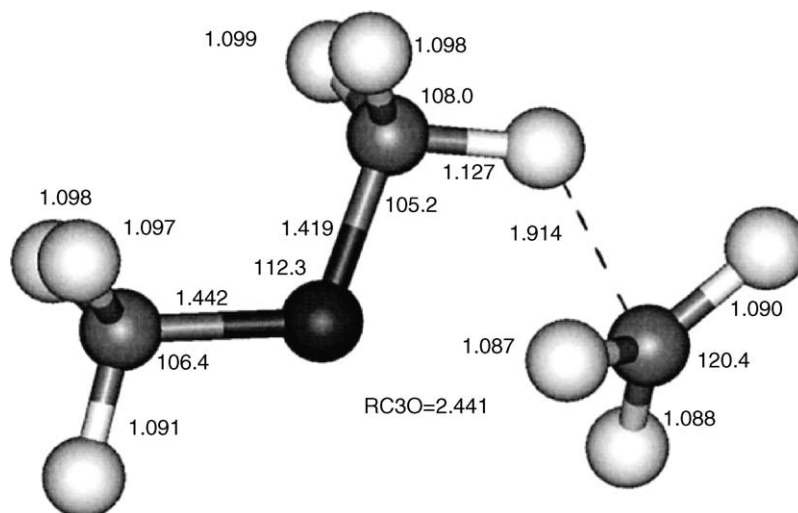


Fig. 1. Transition state obtained by QCISD/6-31G\* theory for the elimination of methane from  $(\text{CH}_3)_3\text{O}^+$ . C3 is the carbon of the mobile methyl. Note that the methyl is a long way from both the oxygen it is leaving and the hydrogen it is acquiring, whereas the CH bond to the hydrogen being transferred is only slightly elongated. Thus the reaction is highly asynchronous.

angles of  $113.6^\circ$  and CO bond lengths of  $1.484 \text{ \AA}$ . One hydrogen of each methyl is nearly parallel to the  $\text{C}_3$  axis and pointing in the opposite direction from the lone electron pair on the oxygen. These hydrogens have CH bond lengths of  $1.039 \text{ \AA}$  and HCO bond angles of  $108.8^\circ$ . The other two hydrogens on each carbon are on the opposite side of the ion with CH bond lengths of  $1.090 \text{ \AA}$  and HCO bond angles of  $106.2^\circ$ .

The trajectories taken by key atoms during elimination of  $\text{CH}_4$  from  $(\text{CH}_3)_3\text{O}^+$  along the minimum energy pathway were characterized by transition state finding and intrinsic reaction coordinate (IRC) [19,20] routines. The transition state is depicted in Fig. 1. During methane elimination from  $(\text{CH}_3)_3\text{O}^+$ , a CO bond stretches from  $1.484 \text{ \AA}$  in the ground state to  $2.441 \text{ \AA}$  at the transition state (QCISD/6-31G\* theory). As it leaves the oxygen, the migrating methyl begins to approach a hydrogen ( $\text{H}_t$ ) on another methyl (The  $\text{CH}_t$  distance equals  $1.914 \text{ \AA}$  at the transition state), and the original  $\text{CH}_t$  bond lengthens slightly from  $1.090$  to  $1.127 \text{ \AA}$  (Fig. 1). Thus C–O bond breaking largely occurs before and transfer of  $\text{H}_t$  occurs mostly after the transition state is passed, confirming that the reaction is highly asynchronous. Interestingly, transition states for HX elimination from neutral haloethanes have similar geometries to the one just described, with a greatly extended C–X bond ( $2.0$ – $3.4 \text{ \AA}$ ), some interaction between X and  $\text{H}_t$ , and some extension of the C– $\text{H}_t$  bond [21–24].

There is little rotation in any direction of the itinerant methyl over the entire course of the reaction, as the distances between the hydrogens on that methyl and the carbon bearing  $\text{H}_t$  change little between the ground and transition state (10%,  $-8\%$  and  $-1\%$ ). This is demonstrated after the transition state by two of the HCOC dihedral angles that each include one hydrogen in the shifting methyl, the carbon of the shifting methyl, the oxygen and the carbon in the remaining methyl varying only by  $18.2^\circ$  and  $9.9^\circ$  between the transition state and the dissociated products (IRC calculations). The third HCOC dihedral bond angle changes from  $-123.0^\circ$  at the transition state to  $-174.8^\circ$

over the same segment of the reaction coordinate. This larger change is largely due to accommodation of the addition of the fourth hydrogen to the carbon rather than to twisting of the methyl/methane. Simultaneously, the methyl carbon goes from being  $155^\circ$  to  $95^\circ$  to the CO double bond at a point  $0.52 \text{ \AA}$  from the oxygen and  $0.89 \text{ \AA}$  from the carbon of that bond. The methane carbon moves steadily away from both termini of the developing double bond after the system passes the transition state. The maintenance of the orientation of the moving methyl to the rest of the ion over the course of the reaction contrasts with the rolling over of methyls observed in the course of two other methane elimination reactions considered to involve ion-neutral complex intermediates [3,25]. The ability of at least one partner to flip over relative to the other is a criterion for the existence of an ion-neutral complex [26], one that the present system does not fulfill on its minimum energy pathway.

## 2.2. Charge distribution and bonding

At the (B3LYP/6-311G\*\*) transition state, the total charge on the migrating methyl is  $0.72$  (natural population analysis) to  $0.68$  (Mulliken charge distributions). In previous methane eliminations from cation radicals through ion-neutral complexes containing methyl radicals, charge was more concentrated on one partner (97% on  $\text{CH}_3\text{O}^+=\text{CHCH}_3$  in the elimination of methane from ionized isopropyl methyl ether [27] and 91–97% on the isopropyl moiety in  $[(\text{CH}_3)_2\text{CH}^+ \cdot \text{CH}_3]$  complexes leading to  $\text{CH}_4$  elimination [28]). Thus the charge is much more distributed over both incipient fragments of  $(\text{CH}_3)_3\text{O}^+$  than would be expected if the transition state were an ion-neutral complex, and the CO bond is cleaving heterolytically, as it must to produce  $\text{CH}_3\text{OCH}_3 + ^+\text{CH}_3$  from  $(\text{CH}_3)_3\text{O}^+$ . (These products, but not the higher energy  $\text{CH}_3\text{OCH}_3^{\bullet+} + \cdot\text{CH}_3$  pair, are produced by dissociation of  $(\text{CH}_3)_3\text{O}^+$ .) Initiation of heterolytic cleavage of  $(\text{CH}_3)_3\text{O}^+$  in methane elimination from  $(\text{CH}_3)_3\text{O}^+$  was suggested previously [17].

According to the Mulliken overlap population, there is essentially no CO bond to the migrating methyl at the transition state. Theory places this population in the range  $-0.00646$  (QCISD/6-31G<sup>\*</sup>) to  $0.02568$  (B3LYP/6-311G<sup>\*\*</sup>), so the CO covalent bond essentially disappears before the transition state is reached. Corresponding values are  $0.26047$  and  $0.38436$  for the CO bond in the ground state of  $(\text{CH}_3)_3\text{O}^+$ . However, the  $\text{CH}_t$  overlap population,  $0.08400$  (QCISD/6-31G<sup>\*</sup>) to  $0.1066$  (B3LYP/6-311G<sup>\*\*</sup>), demonstrates some binding of the C with  $\text{H}_t$  at the transition state. The breaking  $\text{CH}_t$  bond is beginning to weaken at the transition state, as the Mulliken overlap in that bond at the transition state is  $0.624367$  (QCISD/6-31G<sup>\*</sup>) to  $0.67851$  (B3LYP/6-311G<sup>\*\*</sup>), lower than corresponding values of  $0.70865$  and  $0.80092$  for the overlap in another CH bond to the same carbon at the same levels of theory. The transition states for elimination of HX from haloethanes are similar to the ones just described; they have little to no C–X bonding, more  $\text{H}_t\text{X}$  bonding and considerable remaining  $\text{H}_t\text{C}$  bonding [21,23].

The large distances at the transition state of the methyl from both the oxygen it is leaving and the hydrogen it is abstracting confirm the supposition of Wang et al. [17] that the transition state strongly resembles a  $[\text{CH}_3^+(\text{CH}_3)_2\text{O}]$  complex. However, the distribution of charge between the fragments and the overlap population in the  $\text{CH}_t$  bond at the transition state demonstrates that the developing fragments are held together in part by covalent attractions, i.e., the transition state is not an ion-neutral complex as defined above.

### 2.3. Energies of stationary points

The energies of pertinent stationary points on the  $\text{C}_3\text{H}_9\text{O}^+$  potential surface obtained at several levels of theory are given in

Table 1  
Energies of stationary points on the  $\text{C}_3\text{H}_9\text{O}^+$  potential surface

	$(\text{CH}_3)_3\text{O}^+$	TS(–CH <sub>4</sub> )	$(\text{CH}_3)_2\text{O}$	$^+\text{CH}_3$	$\text{CH}_3\text{O}^+=\text{CH}_2$	$\text{CH}_4$
B3LYP/6-31G <sup>*a</sup>	–194.657241	–194.550413	–155.025051	–39.480387	–154.112475	–40.518313
B3LYP/6-311G <sup>**</sup>	–194.711716	–194.607948	–155.071928	–39.491365	–154.155033	–40.533748
QCISD/6-31G <sup>*</sup>	–194.034415	–193.919848	–154.538618	–39.345965	–153.653945	–40.353370
QCISD(T)/6-311G <sup>**</sup>	–194.199833	–194.086260	–154.668086	–39.381142	–153.767611	–40.405948
//QCISD//6-31G <sup>*b</sup> QCISD(T)/6-311+G <sup>**</sup>	–194.204802	–194.092713	–154.675664	–39.381280	–153.770655	–40.401976
//QCISD//6-31G <sup>*b</sup> ZPVE	314.3	294.7	206.8	81.4	178.1	116.4
	Relative energies					
	TS(–CH <sub>4</sub> )	$(\text{CH}_3)_2\text{O} + ^+\text{CH}_3$	$\text{CH}_3\text{O}^+=\text{CH}_2 + \text{CH}_4$	$(\text{CH}_3)_3\text{O}^+$		
B3LYP/6-31G <sup>*</sup>	260.9	372.5	49.5	0		
B3LYP/6-311G <sup>**</sup>	252.8	363.6	40.4	0		
QCISD/6-31G <sup>*</sup>	281.2	367.3	51.4	0		
QCISD(T)/6-311G <sup>**</sup>	278.6	369.3	49.2	0		
QCISD(T)/6-311+G <sup>**</sup>	274.7	362.2	64.7	0		
Experimental <sup>c</sup>	909.3 (366)	582.5 (60)	523 <sup>d</sup> (0)			

<sup>a</sup>  $(\text{CH}_3)_3\text{O}^+$  could only be optimized at the B3LYP/6-31G<sup>\*</sup> level by including the command INT = ULTRAFINE. Therefore all B3LYP results presented in this table were obtained with inclusion of the ULTRAFINE command. The QCISD and QCISD(T) calculations were unaffected by this problem.

<sup>b</sup> Optimum geometries and energies for other species were calculated at the same levels of theory, but the energies for these species were obtained by applying QCISD(T)/6-311G<sup>\*\*</sup> and QCISD(T)/6-311+G<sup>\*\*</sup> theories to QCISD/6-31G<sup>\*</sup> geometries.

<sup>c</sup> Based on the following values obtained from Ref. [29]:  $\text{CH}_3\text{OCH}_3$  –184.0,  $^+\text{CH}_3$  1093.3,  $\text{CH}_3\text{O}^+=\text{CH}_2$  657,  $\text{CH}_4$  –74.5. The values in parentheses are differences between product and reactant heats of formation.

<sup>d</sup> From Ref. [17].

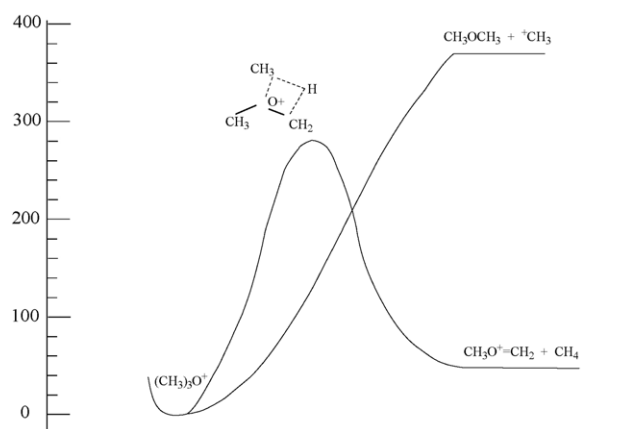


Fig. 2. Potential energy diagram for the elimination of methane and the formation of  $\text{CH}_3^+ + \text{CH}_3\text{OCH}_3$  from  $(\text{CH}_3)_3\text{O}^+$ . Energies were obtained by QCISD(T)/6-311G<sup>\*\*</sup>//QCISD/6-31G<sup>\*</sup> theory.

Table 1, and a potential diagram in Fig. 2 summarizes those energies from QCISD(T)/6-311G<sup>\*\*</sup>//QCISD/6-31G<sup>\*</sup> theory. The transition state for methane elimination is  $210\text{--}230\text{ kJ mol}^{-1}$  above the thermochemical threshold for this elimination and in the range  $86\text{ kJ mol}^{-1}$  (QCISD/6-31G<sup>\*</sup>) to  $91\text{ kJ mol}^{-1}$  (QCISD(T)/6-311G<sup>\*\*</sup>) below the energy required for dissociation to  $^+\text{CH}_3 + \text{CH}_3\text{OCH}_3$ . The computed differences between the thresholds for the losses of methyl and of methane are somewhat larger than the  $30 \pm 30\text{ kJ mol}^{-1}$  previously derived from experimental data [17]. The consistency of our values across levels of theory supports their reasonable accuracy.

A transition state for  $^+\text{CH}_3$  formation from  $(\text{CH}_3)_3\text{O}^+$  with an energy of  $-194.537774$ , a ZPVE of  $286.6\text{ kJ/mol}$  and an energy of  $286.0\text{ kJ mol}^{-1}$  above that of  $(\text{CH}_3)_3\text{O}^+$  was located

by B3LYP/6-31G\* theory. Several attempts to find this TS at the B3LYP/6-311G\*\* level and an attempt at the QCISD/6-31G\* level failed. Thus it is doubtful that such a potential maximum occurs on the reaction coordinate for simple dissociation, and the threshold for dissociation is likely at the energy of the products (Table 1).

#### 2.4. The reaction coordinate

The reaction coordinate for the elimination of methane from (CH<sub>3</sub>)<sub>3</sub>O<sup>+</sup> might be expected to be quite similar to that for elimination of the elements of methane from (CH<sub>3</sub>)<sub>4</sub>N<sup>+</sup>. However, the two reactions instead contrast markedly in that the former is a CH<sub>4</sub> elimination and the latter is a loss of CH<sub>3</sub> followed by H [13]. The latter is attributable to the threshold for methane elimination being above that for methyl loss, opposite to the order for (CH<sub>3</sub>)<sub>3</sub>O<sup>+</sup>. However, we also found a higher energy transition state for methane elimination from (CH<sub>3</sub>)<sub>4</sub>N<sup>+</sup> with properties similar to the transition state described above for methane elimination [13]. The latter transition state is probably largely inoperative due to its higher energy.

The elimination of CH<sub>4</sub> from (CH<sub>3</sub>)<sub>3</sub>O<sup>+</sup> is a rare example in a closed shell ion of a 1,2-elimination in which a methyl migrates to a hydrogen in the course of the dissociation, although similar H migrations are common in 1,2-H<sub>2</sub>-eliminations [1]. As in the elimination of CH<sub>4</sub> from CH<sub>3</sub>CH=OH<sup>+</sup>, the parallel formation of <sup>+</sup>CH<sub>3</sub> + CH<sub>3</sub>OCH<sub>3</sub> has a much higher thermochemical threshold than does the elimination of CH<sub>4</sub>. The thresholds for cleavage of C–X bonds in haloalkanes are also much higher than the energies of the HX + C<sub>2</sub>H<sub>4</sub> products, and their reaction coordinates are similar to that for methane elimination from (CH<sub>3</sub>)<sub>3</sub>O<sup>+</sup> described here [21,24]. The preceding indicates that the suggestion [3,14] that high energy eliminations can occur by concerted but highly non-synchronous transition states is fairly general.

In perhaps the first effort to understand the high barriers to 1,2-eliminations from ions in the gas phase, Williams and Hvistendahl attributed those barriers to the associated processes being forbidden by orbital symmetry [30]. However, Uggerud later stated that it is very difficult to predict by Woodward–Hoffmann theory whether an elimination will have a 1,1- or a 1,2-transition state, advocating instead the use of frontier orbital theory [1]. We have concluded [5,6] based on our studies that the varied mechanisms of formal 1,2-eliminations from cations [1–6,13–16] arise from them being forced into channels that avoid violating the constraints of orbital symmetry. The similarity of the geometries of the transition states for eliminations of HX from neutral haloethanes [21–24] to those found for cations in this work and elsewhere [1] demonstrates that asynchronous but concerted transition states for 1,2-eliminations are common, probably the rule, when the threshold for simple cleavage is much higher than the energy of the elimination products.

### 3. Theory

All calculations were performed using the Gaussian 03 program package [18]. Geometries were obtained by QCISD/6-

31G\*, B3LYP/6-31G\* and B3LYP/6-311G\*\* theories. Energies were obtained at the geometries obtained at the same level of theory, except for QCISD(T)/6-311G\*\*//QCISD/6-31G\* and QCISD(T)/6-311+G\*\*//QCISD/6-31G\* energies. The similarity between the values produced by the last two levels of theory demonstrate that it was not necessary to use diffuse functions to obtain reasonable energies. Stable species at energy minima were identified by having only positive vibrational frequencies, and points with one imaginary vibrational frequency were considered to be transition states. Reaction pathways were traced by IRC methods [19,20] with a B3LYP/6-31G\* basis set. Zero point energies were obtained by multiplying those derived from B3LYP/6-31G\* frequencies by the scaling factor 0.9806 [31]. Relative energies were consistent within 20 kJ mol<sup>-1</sup> across levels of theory and were therefore reasonable (Table 1).

### References

- [1] E. Uggerud, *Mass Spectrom. Rev.* 18 (1999) 285.
- [2] D.J. McAdoo, R.D. Bowen, *Eur. Mass Spectrom.* 5 (1999) 389.
- [3] C.E. Hudson, D.J. McAdoo, *Int. J. Mass Spectrom.* 232 (2004) 17.
- [4] C.E. Hudson, D. Wang, D.J. McAdoo, *Int. J. Mass Spectrom.* 236 (2004) 105.
- [5] C.E. Hudson, D.J. McAdoo, *J. Am. Soc. Mass Spectrom.* 9 (1998) 138.
- [6] C.E. Hudson, S. Eapen, D.J. McAdoo, *Int. J. Mass Spectrom.* 228 (2003) 955.
- [7] R.B. Woodward, R. Hoffmann, *Angew. Chem.* 8 (1967) 781.
- [8] T.H. Morton, *Tetrahedron* 38 (1982) 3195.
- [9] D.J. McAdoo, *Mass Spectrom. Rev.* 7 (1988) 363.
- [10] R.D. Bowen, *Accts. Chem. Res.* 24 (1991) 364.
- [11] P. Longevialle, *Mass Spectrom. Rev.* 11 (1992) 157.
- [12] D.J. McAdoo, T.H. Morton, *Accts. Chem. Res.* 26 (1993) 295.
- [13] C.E. Hudson, L.L. Griffin, D.J. McAdoo, *Eur. J. Mass Spectrom.* 10 (2004) 767.
- [14] C.E. Hudson, L. DeLeon, D. Van Alstyne, D.J. McAdoo, *J. Am. Soc. Mass Spectrom.* 5 (1994) 1102.
- [15] E.L. Øiestad, Å.M.L. Øiestad, H. Skaane, K. Ruud, T. Helgaker, E. Uggerud, *Eur. Mass Spectrom.* 1 (1995) 121.
- [16] Å.M.L. Øiestad, E. Uggerud, *Int. J. Mass Spectrom. Ion Process.* 167/168 (1997) 117.
- [17] D. Wang, R.R. Squires, D. Fărcasiu, *Int. J. Mass Spectrom. Ion Process.* 107 (1991) R7.
- [18] M.J. Frisch, G.W. Trucks, H.B. Schlegel, G.E. Scuseria, M.A. Robb, J.R. Cheeseman, J.A. Montgomery Jr., T. Vreven, K.N. Kudin, J.C. Burant, J.M. Millam, S.S. Iyengar, J. Tomasi, V. Barone, B. Mennucci, M. Cossi, G. Scalmani, N. Rega, G.A. Petersson, H. Nakatsuji, M. Hada, M. Ehara, K. Toyota, R. Fukuda, J. Hasegawa, M. Ishida, T. Nakajima, Y. Honda, O. Kitao, H. Nakai, M. Klene, X. Li, J.E. Knox, H.P. Hratchian, J.B. Cross, C. Adamo, J. Jaramillo, R. Gomperts, R.E. Stratmann, O. Yazyev, A.J. Austin, R. Cammi, C. Pomelli, J.W. Ochterski, P.Y. Ayala, K. Morokuma, G.A. Voth, P. Salvador, J.J. Dannenberg, V.G. Zakrzewski, S. Dapprich, A.D. Daniels, M.C. Strain, O. Farkas, D.K. Malick, A.D. Rabuck, K. Raghavachari, J.B. Foresman, J.V. Ortiz, Q. Cui, A.G. Baboul, S. Clifford, J. Cioslowski, B.B. Stefanov, G. Liu, A. Liashenko, P. Piskorz, I. Komaromi, R.L. Martin, D.J. Fox, T. Keith, M.A. Al-Laham, C.Y. Peng, A. Nanayakkara, M. Challacombe, P.M.W. Gill, B. Johnson, W. Chen, M.W. Wong, C. Gonzalez, J.A. Pople, *Gaussian 03, Revision B.04*, Gaussian, Inc., Pittsburgh PA, 2003.
- [19] C. Gonzalez, H.B. Schlegel, *J. Chem. Phys.* 90 (1989) 2154.
- [20] C. Gonzalez, H.B. Schlegel, *J. Phys. Chem.* 94 (1990) 5523.
- [21] J.L. Toto, G.O. Pritchard, B. Kirtman, *J. Phys. Chem.* 98 (1994) 8359.
- [22] K.B. Børve, V.R. Jensen, *J. Chem. Phys.* 105 (1996) 6910.

- [23] T. Thorsteinsson, A. Famulari, M. Raimondi, *Int. J. Quant. Chem.* 74 (1999) 231.
- [24] M.P. McGrath, F.S. Rowland, *J. Phys. Chem. A* 106 (2002) 8191.
- [25] C.E. Hudson, D.J. McAdoo, *Int. J. Mass Spectrom.* 199 (2000) 41.
- [26] T.H. Morton, *Org. Mass Spectrom.* 27 (1992) 353.
- [27] S. Olivella, A. Solé, D.J. McAdoo, L.L. Griffin, *J. Am. Chem. Soc.* 116 (1994) 11078.
- [28] S. Olivella, A. Solé, D.J. McAdoo, L.L. Griffin, *J. Am. Chem. Soc.* 117 (1995) 2557.
- [29] S.G. Lias, J.E. Bartmess, J.F. Liebman, J.L. Holmes, R.D. Levin, W.G. Mallard, *J. Phys. Chem. Ref. Data* 17 (Suppl. 1) (1988).
- [30] D.H. Williams, G. Hvistendahl, *J. Am. Chem. Soc.* 96 (1974) 6753.
- [31] A.P. Scott, L. Radom, *J. Phys. Chem.* 100 (1996) 16502.